7-2013

Computational renormalization scheme for quantum field theories

Rainer Grobe
Illinois State University

Qichang Su
Illinois State University

R E. Wagner
Illinois State University

Computational renormalization scheme for quantum field theories

R. E. Wagner, Q. Su, and R. Grobe
Intense Laser Physics Theory Unit and Department of Physics, Illinois State University, Normal, Illinois 61790-4560, USA
(Received 11 March 2013; published 15 July 2013)

We propose an alternative technique for numerically renormalizing quantum field theories based on their Hamiltonian formulation. This method is nonperturbative in nature and, therefore, exact to all orders. It does not require any correlation functions or Feynman diagrams. We illustrate this method for a model Yukawa-like theory describing the interaction of electrons and positrons with model photons in one spatial dimension. We show that, after mass renormalization of the fermionic and bosonic single-particle states, all other states in the Fock space have finite energies, which are independent of the momentum cutoff.

DOI: 10.1103/PhysRevA.88.012113 PACS number(s): 03.65.−w

I. INTRODUCTION

The studies of quantum electrodynamical systems usually rely on perturbative expansions of the S matrix and Green's functions in order to make the problem tractable [1–9]. S-matrix-based treatments have the drawback that they cannot provide any space- or time-resolved information concerning the dynamics inside the interaction zone. On the other hand, space-time resolved, *ab initio* studies of quantum-field-theoretical systems may help to shed light on many problems that require a field-theoretical treatment. In contrast to the traditional asymptotic in-out formalism [10,11] of the S-matrix-based approaches, these *ab initio* simulations are based on the quantum-field-theoretical Hamiltonian and describe the time evolution of an initial state inside the interaction zone. The time-evolved state is then used to compute various observables such as expectation values or spatial, momentum, or energy densities or their correlations. These simulations have already been proven to be useful in the understanding of some quantum systems [12], including the role of force-mediating bosons for interfermionic forces [13], the dynamical impact of mass dressing [14], or time-resolved studies of the absorption of photons by electrons in model Compton scattering systems [15].

Nonperturbative, *ab initio* numerical simulations have been undertaken based on both scalar field theory with ϕ^2 or ϕ^4 interactions [16] and Yukawa-like fermion-boson systems [17]. However, the field theories in these prior studies did not have any ultraviolet singularities and the required renormalization was finite, either due to low dimensionality or the lack of an antifermion in the case of Yukawa theory. In order to move beyond such model systems and develop numerical techniques for more complex systems such as full QED, as a first step it is necessary to find a new renormalization technique that can be applied directly to the Hamiltonian instead of the S-matrix.

In this paper we demonstrate such a renormalization technique and illustrate it for a Yukawa-like model system representing the interaction of electrons and positrons with model photons (e.g., spinless bosons with finite mass). The energy spectrum of the original Hamiltonian does not converge as the largest momentum in the system or the length of the numerical box are increased. In the traditional renormalization [18–25] framework based on perturbation theory [26], divergences can be removed order-by-order only by adding diverging counterterms to the corresponding Lagrangian [27], but our nonpertubative Hamiltonian approach allows us to renormalize the spectrum to all orders.

We introduce here a computational method that can remove any divergence from the spectrum by calculating the diverging bare mass parameters in the Hamiltonian directly, such that the resulting spectrum becomes independent of the maximum momentum or the physical size of the numerical box. By repeatedly diagonalizing the Hamiltonian, this algorithm iteratively updates the bare parameters of the Hamiltonian until the correct physical energies of the single-particle states are achieved. These bare parameters are functions of the maximum momentum and the numerical box size and depend, of course, on the desired values of the physical mass and the given coupling constant. We show that once the correct bare parameters have been found for the single-particle states, other multiparticle states are automatically convergent and divergence-free. In this way, the time evolution of any initial state and the properties of all multiparticle states then can be studied without any further approximation or constraint.

To illustrate this technique for a concrete example, we use a Yukawa theory with the usual electrons and positrons as well as a theory with neutral Majorana fermions [28]. Previous numerical simulations of Yukawa theory were based on a version of the theory that did not contain positrons; however, the work presented here differs in that electron-positron pair creation processes are allowed in the present paper, while in previous work fermions could only radiate or absorb photons and the number of fermions was conserved.

This paper is organized as follows. In Sec. II we briefly review the derivation of the two Hamiltonian model systems from their Lagrangain densities. In Sec. III we show how the Hilbert space can be truncated to allow for a computational analysis and discuss a numerical method for space- and time-resolved studies of a quantum field theory. In Sec. IV we analyze the divergence of the energy spectrum before mass renormalization in the perturbative and nonperturbative regimes. In Sec. V we introduce the proposed iterative numerical renormalization algorithm and apply it to the single-particle energies in the perturbative regime. In Sec. VI we demonstrate that the technique can also remove the divergences for all states in the spectrum, even in the strong-coupling, nonperturbative regime, as shown in Sec. VII. Finally, in Sec. VIII we conclude with a summary, a critical discussion, and an outlook on future work.

II. THE FIELD-THEORETICAL MODEL HAMILTONIANS

The first model system we consider is the Yukawa fermion-boson system with a real scalar field ϕ and a Dirac electron-positron field operator ψ_D. The Lagrangian density for this system is given by

$$L_D = c\bar{\psi}_D(x)\,(i\gamma^\mu\partial_\mu - M)\,\psi_D(x) + 1/2\,\partial_\mu\phi(x)\,\partial^\mu\phi(x) - 1/2(mc)^2\,\phi(x)^2 - \lambda c^{3/2}\,\bar{\psi}_D(x)\,\psi_D(x)\,\phi(x), \quad (2.1)$$

where M and m are the bare mass parameters for the electron and photon, respectively, and $\bar{\psi}_D = \psi_D^\dagger\gamma^0$. From now on we use atomic units. Because we restrict our attention to only one spatial dimension, we may choose to examine only a single spin direction of the electron and positron. In this way we only need a two-component spinor to represent the fermions. This allows us to choose gamma matrices $\gamma^0 = \sigma^3$ and $\gamma^1 = \sigma^1$, while the derivative is given by $\partial_\mu = (1/c\,\partial_t, \partial_z)$. The (model) photon and electron-positron field operator can be expanded in terms of the usual momentum mode operators as

$$\phi(x) = \int dk\, c\,(4\pi\omega_k)^{-1/2}\,(a_k\,e^{ikx} + a_k^\dagger e^{-ikx}), \quad (2.2a)$$

$$\psi_D(x) = \int dp\,(2\pi)^{-1/2}\,(b_p\,u_p\,e^{ipx} + d_p^\dagger\,v_p\,e^{-ipx}). \quad (2.2b)$$

Here a_k and $a_k^\dagger$ are the creation and annihilation operators for the boson; b_p and $b_p^\dagger$ are the creation and annihilation operators for the electron; d_p and $d_p^\dagger$ are the corresponding positron operators; ω_k is the energy of a model photon with momentum k, $\omega_k = \sqrt{(m^2c^4 + c^2k^2)}$; E_p is the energy of an electron with momentum p, $E_p = \sqrt{(M^2c^4 + c^2p^2)}$; and u_p and v_p are the positive and negative energy solutions, respectively, to the Dirac equation, where u_p takes the form $u_p = (1 + \{pc/[Mc^2 + E(p)]\}^2)^{-1/2}\,(1,\, pc/[Mc^2 + E(p)])^T$. Here and throughout this paper, boson momentum modes will be denoted by k and fermion momentum modes by p.

The Hamiltonian for this system, written in terms of the creation and annihilation operators, is then given by

$$H_D = \int dp\,E_p\,b_p^\dagger b_p + \int dp\,E_p\,d_p^\dagger d_p + \int dk\,\omega_k\,a_k^\dagger a_k + V_D, \quad (2.3a)$$

$$V_D = \lambda\,c^{5/2}\int dp\int dk\,(16\,\pi^3\,\omega_k)^{-1/2}\,[\bar{u}_{p+k}u_p\,b_{p+k}^\dagger \times b_p\,(a_k + a_{-k}^\dagger) + \bar{u}_{p+k}v_{-p}\,b_{p+k}^\dagger\,d_{-p}^\dagger\,(a_k + a_{-k}^\dagger) + \bar{v}_{-p}u_{p+k}\,b_{p+k}\,d_{-p}\,(a_{-k} + a_k^\dagger) + \bar{v}_p v_{p+k}\,d_{p+k}^\dagger\,d_p \times (a_k + a_{-k}^\dagger)], \quad (2.3b)$$

where $\bar{u}_p = u_p^\dagger\,\gamma^0$ and similarly for $\bar{v}_p$.

In addition to the standard Yukawa theory with a real scalar and a Dirac spinor field, we will also investigate below a Yukawa-type theory with Majorana fermions. The Majorana condition imposes a kind of reality on the fermion field which, similarly to a real scalar boson, makes the Majorana fermion its own antiparticle. The Lagrangian density for a Yukawa system with a Majorana fermion is given by

$$L_M = 1/2\,c\,\bar{\psi}_M(x)\,(i\gamma^\mu\partial_\mu - M)\,\psi_M(x) + 1/2\,\partial_\mu\phi(x)\,\partial^\mu\phi(x) - 1/2(mc)^2\,\phi(x)^2 - 1/2\,\lambda\,c^{3/2}\,\bar{\psi}_M(x)\,\psi_M(x)\,\phi(x). \quad (2.4)$$

The factor of $\frac{1}{2}$ on the fermion kinetic terms is necessary to give the Majorana fermion the correct energy, since the field operator has only half as many degress of freedom, while the factor of $\frac{1}{2}$ in the interaction term ensures that the fermion-boson coupling has the proper strength, as will become clear when the Hamiltonian is written in terms of the mode operators below. The boson field ϕ is the same in the Majorana theory as it is for the standard Yukawa theory [see Eq. (2.2a)], while the fermion field now only contains one kind of creation or annihilation operator,

$$\psi_M(x) = \int dp\,(2\pi)^{-1/2}\,(f_p\,u_p\,e^{ipx} + f_p^\dagger\,v_p\,e^{-ipx}), \quad (2.5)$$

where $f_p^\dagger$ and f_p are the creation and annihilation operators for the Majorana fermion. The Majorana Hamiltonian, when expressed in terms of the creation and annihilation operators, is

$$H_M = \int dp\,E_p\,f_p^\dagger\,f_p + \int dk\,\omega_k\,a_k^\dagger a_k + V_M, \quad (2.6a)$$

$$V_M = \lambda\,c^{5/2}\int dp\int dk\,(16\,\pi^3\,\omega_k)^{-1/2}\,[\bar{u}_{p+k}u_p\,f_{p+k}^\dagger\,f_p \times (a_k + a_{-k}^\dagger) + 1/2\,\bar{u}_{p+k}v_{-p}f_{p+k}^\dagger\,f_{-p}^\dagger\,(a_k + a_{-k}^\dagger) + 1/2\,\bar{v}_{-p}u_{p+k}\,f_{p+k}\,f_{-p}\,(a_{-k} + a_k^\dagger)]. \quad (2.6b)$$

As seen here, the Majorana Hamiltonian is nearly the same as the Yukawa theory with Dirac fermions, except for the obvious absence of antiparticle terms, the replacement of antiparticle creation and annihilation operators with their counterpart, and the appearance of a factor of $1/2$ on the pair creation $f_{p+k}^\dagger f_{-p}^\dagger(a_k + a_{-k}^\dagger)$ and annihilation $f_{p+k}f_{-p}(a_{-k} + a_k^\dagger)$ terms. The choice of this factor of $1/2$ is necessary in order to ensure that the interaction term for the radiation or absorption of a boson by the fermion in Eq. (2.6b), $\bar{u}_{p+k}u_p\,f_{p+k}^\dagger\,f_p\,(a_k + a_{-k}^\dagger)$, has the same strength as the equivalent term for the Dirac fermion in Eq. (2.3b).

III. NUMERICAL CONSIDERATIONS FOR THE HILBERT SPACE

In order to study the time evolution of quantum-field-theoretical systems, we need to compute the quantum-field-theory state $|\Phi(t)\rangle$ from a given initial state $|\Phi(0)\rangle$. The time evolution follows a Schrödinger-like differential equation, $i\,\partial/\partial t|\Phi(t)\rangle = H|\Phi(t)\rangle$, where the Hamiltonian H is either H_D for the Yukawa theory with electrons and positrons or H_M for Majorana fermions. This can be accomplished by numerically diagonalizing the Hamiltonian and finding the energy eigenstates and eigenenergies. Once these eigenstates are identified, it is straightforward to decompose the initial state $|\Phi(0)\rangle$ into its eigenstate components (whose time evolution is simple) and then reconstruct the state $|\Phi(t)\rangle$ at any time t.

In order to diagonalize the Hamiltonians Eqs. (2.3) and (2.6), the particles' momenta must first be discretized by placing the system within a finite box of length L and imposing periodic boundary conditions [29]. Furthermore, the fermion's momentum mode is limited to lie below an integer cutoff $P_{\max}$, $|p/\Delta p| < P_{\max}$, where p is the momentum of the fermion and Δp is the gap between the discretized momentum modes, $\Delta p = 2\pi/L$. Likewise, the boson momentum modes are constrained by $|k/\Delta p| < P_{\max}$. From now on we denote the largest available momentum as $\Lambda \equiv P_{\max}\Delta p$.

The eigenenergies of the Hamiltonian do not converge as $P_{\max}$ approaches infinity. This momentum cutoff, which must be introduced to make the Fock space finite dimensional so the problem becomes numerically tractable, also serves as a cutoff to regulate otherwise divergent integrals. The focus of the renormalization program, presented below, is to ensure that the (renormalized) Hamiltonian correctly predicts the physically measurable observables (electron, positron, and boson masses), which should no longer depend on the cutoff $P_{\max}$.

Even when the momentum is discretized and the particles' momenta are restricted to lie below some cutoff, the Fock space is still infinite dimensional because an infinite number of bosons can occupy any given momentum mode. In order to rectify this, and also in order to keep the Fock space small enough to fall within the constraints imposed by computer memory, the total number of bosons in each Fock space state is limited to at most N_b. Likewise, the number of fermion pairs is limited to at most N_{fp}; here, "fermion pairs" refers to electron-positron pairs in the case of Dirac fermions and fermion-fermion pairs for the Majorana theory.

The diagonalization of the Hamiltonian is made easier by the fact that the Yukawa theory has a number of symmetries that limit which states can couple to other states. Since the total momentum is conserved, states with different momenta cannot couple to one another in the Hamiltonian, which makes the Hamiltonian block diagonal. Each momentum block therefore can be diagonalized independently of the other blocks. Furthermore, as the total charge is conserved in the Yukawa theory for Dirac fermions, the fermion number N_L, defined as the number of electrons minus the number of positrons, is conserved. Thus, each state only couples to other states where the difference between the number of electrons and positrons is identical, which similarly makes the Hamiltonian block diagonal. In the Majorana theory, there is no conserved fermion number; however, fermions can be created or destroyed only in pairs, and, thus, states with an odd number of fermions cannot couple to states with an even number of fermions in the Majorana theory.

In order to obtain numerically converged data, we have used up to 9000 Fock space states in a single momentum block in the Hamiltonian. It should be noted that a theory with Majorana fermions is more numerically tractable than the Yukawa theory with Dirac fermions because the number of Fock space states is substantially reduced, especially for states with large numbers of fermions. This difference in the number of states between the two kinds of fermions exists because Majorana fermions are indistinguishable while electrons are distinguishable from positrons. Quantum states with Majorana fermions therefore are divided by larger combinatorical factors to avoid overcounting of identical particles. For instance, for $P_{\max} = 10$, the total number of states with zero total momentum which contain four Majorana fermions is only 218, while the total number of states with two Dirac fermions and two Dirac antifermions is 1462. The smaller number of states in the Majorana theory makes it possible to explore parameter regimes which are inaccessible in the Dirac theory due to memory constraints; in particular, in the Majorana theory we are able to explore higher-momentum cutoffs, the nonperturbative coupling regime, and multiparticle states where the number of states in the Dirac theory was too large for present computational capabilities.

IV. ULTRAVIOLET DIVERGENCE OF THE ENERGY SPECTRUM FOR FIXED BARE MASSES *m* AND *M*

The traditional perturbative methods can be used to estimate the type of divergences we could expect for our two Hamiltonians. Power-counting arguments [11] suggest that the superficial degree of divergence for the boson propagator in a Yukawa theory is logarithmically divergent in one spatial dimension, while other diagrams are superficially convergent. Indeed, the one-loop Feynman diagram for the boson propagator diverges, while the one-loop diagram for the fermion propagator remains finite. Mass renormalization of the boson therefore is necessary in order to render the theory finite, and although the fermion propagator does not diverge at lowest order, the fermion mass will still need a *finite* renormalization, since the fermion's dressing from the boson will still cause a mass shift and the physical mass of the fermion will differ by the bare mass parameter by a finite amount, which must be renormalized in order to make the physical mass match the experimentally determined physical mass.

It is important to note that although Feynman diagrams can be used to determine the divergent portion of the integral, they are not sufficient for our purposes as we must also know the finite portion of the renormalization. Various means of regulating and renormalizing a divergent integral can differ from one another by a finite quantity, and this finite difference can depend in particular on shifts in the integration variable when a cutoff regulator is applied. Furthermore, Feynman diagrams can only be used to renormalize a theory order-by-order in perturbation theory, while here we need to develop a numerical technique that is nonperturbative in nature. Nevertheless, such Feynman diagram-based analyses can be useful for setting expectations of the kinds of divergences that exist in the Yukawa theory in the nonperturbative regime of small coupling.

The energy of the Yukawa vacuum, defined as the eigenstate of lowest energy, is not zero, and is, in fact, a negative divergent number with Λ and L. This vacuum energy depends on both $P_{\max}$ and L and does not converge in either limit, $P_{\max} \to \infty$ or $L \to \infty$. There are two reasons for this divergence. First, the perturbative momentum integrals for vacuum bubbles consisting of one boson and two fermions (more specifically an electron and positron in the Dirac case) do not converge. Second, for a box size L that is much larger than the Compton wavelength of the particles, the vacuum's energy becomes proportional to L, and so the energy diverges in the limit $L \to \infty$.

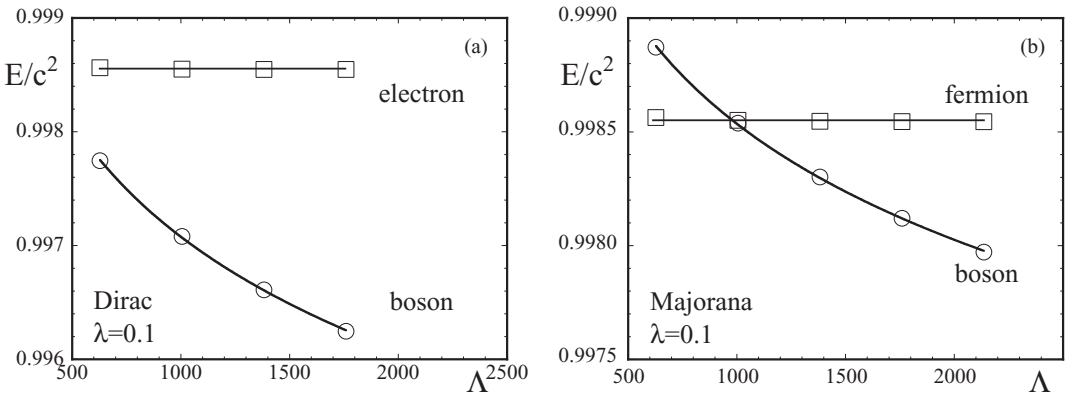

FIG. 1. The rest energy as a function of the cutoff Λ for fixed bare masses ($m = M = 1$). Also plotted is a logarithmic fit to the boson curve and a constant fit to the fermionic curve. In (a), $P_{\max}$ varies from 5 (leftmost data points) to 14 (rightmost data points), In (b), $P_{\max}$ varies from 5 (leftmost) to 17 (rightmost) ($\lambda = 0.1$ and $L = 0.05$. For boson curves, $N_b = 2$ and $N_{\rm fp} = 1$, while for fermion curves $N_b = 1$ and $N_{\rm fp} = 1$).

If the vacuum energy itself is not studied, we can subtract a diverging number from the Hamiltonian such that its energy becomes zero. Loosely speaking, since all physical particles are created "on top of" the underlying vacuum state, all single- and multiparticle states contain the same divergent vacuum energy, and so this energy can be subtracted out from all states in the energy spectrum. Effectively, this means that we must replace the Hamiltonian H by $H - E_{\rm vac}$, where $E_{\rm vac}$ is the divergent vacuum energy. This procedure of subtracting the vacuum energy from all states has been performed throughout all results in this paper, and, thus, when discussing the energy of a particular Fock space state what is meant is the energy of the state above the vacuum energy. As discussed earlier, for the numerical methods presented here the momentum integrals are automatically regulated by a cutoff at a maximum momentum $\Lambda = P_{\max}\,\Delta p$, where $\Delta p = 2\pi/L$ and L is the length of the box.

After the Dirac Hamiltonian H_D or the Majorana Hamiltonian H_M have been diagonalized, it is necessary to locate the states describing a single physical particle within the set of eigenstates so their energies can be determined. As discussed in Sec. II, the Fock space of the Yukawa theory breaks up into separate, noncoupled sectors that can be parametrized by two quantities, the total momentum and the number of fermions and antifermions. In the Dirac theory, the state consisting of a single physical boson at rest must have zero total momentum, $P_{\rm tot} = 0$, and since fermions can only be created in fermion-antifermion pairs, the fermion number $N_L = 0$ as well for the physical boson state, where N_L is the number of fermions minus the number of antifermions. The lowest-lying energy state with $P_{\rm tot} = 0$ and $N_L = 0$ is, of course, the physical vacuum, defined as the state of lowest energy, while the state of a single physical boson will be the second lowest state in this block of states, assuming that the interaction is not so strong as to bring multiparticle bound states down below the energy of single-particle states. Likewise, a single physical fermion at rest has $P_{\rm tot} = 0$ and $N_L = 1$, and since the vacuum has $N_L = 0$ the single physical fermion state will be the lowest energy level of the $P_{\rm tot} = 0$, $N_L = 1$ sector of the Hamiltonian, again assuming that the single-particle state has less energy than other bound states.

Similiarly, the eigenstates of the Majorana theory that correspond to the single physical boson and single physical fermion states can be found by analyzing the spectrum of eigenenergies. For the Majorana theory, there are no antifermions, and states with N_L odd, where N_L is now just the number of fermions, decouple from states with N_L even. The vacuum of the Majorana Yukawa theory will be found in the sector of the Hamiltonian with momentum $P_{\rm tot} = 0$, N_L even, where it will be the state with lowest energy, and the second lowest energy state in this sector will be the state of a single physical boson at rest. Finally, the state of a single physical fermion at rest can be identified as the lowest energy state in the sector of the Majorana Hamiltonian with $P_{\rm tot} = 0$ and N_L odd.

In Fig. 1 the energy of the boson and fermion at rest is examined as a function of the maximum momentum Λ by keeping the bare masses m and M fixed. The coupling $\lambda = 0.1$ is in the perturbative regime.

As expected, for the relatively small, perturbative coupling of $\lambda = 0.1$ in the figure, the energy of the boson diverges in a logarithmic manner, while the fermion energy remains nearly constant for both Dirac and Majorana fermions. The continuous fitted curves are given by $m = 1.0071–0.0015\,\ln\Lambda$ and $m = 1.0036–0.000\,75\,\ln\Lambda$ for the photon in the Dirac and Majorana theory, respectively. Because the coupling in this regime is very weak, expanding the Hilbert space to allow more particles has a negligible effect on these fits, and studies of this issue have shown that increasing N_b and $N_{\rm fp}$ cause the change in the mass (the difference between the mass m and unity) to vary by much less than 1%. A much more significant source of error is the relatively large box size, $L = 0.05$. Studies using perturbation theory, for which very large box lengths are possible, suggest that the difference between the unperturbed and perturbed eigenenergies can vary by as much as 5% as the box size is increased from $L = 0.05$ to an infinite box, $L \to \infty$.

Figure 2 examines single-particle energies for the higher, nonperturbative coupling of $\lambda = 0.7$ in the Majorana theory. For small $P_{\max}$ at this value of λ, it is possible to increase the number of particles included in the Hilbert space N_b and $N_{\rm fp}$, and these investigations indicate that the eigenenergies

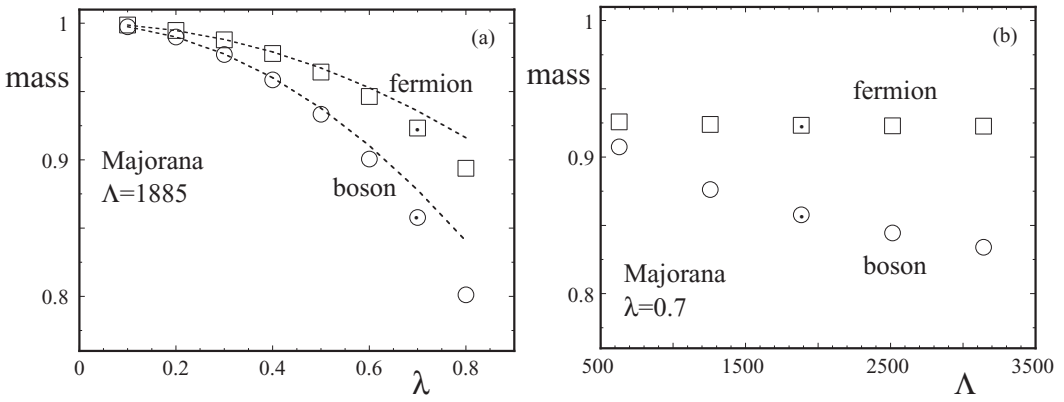

FIG. 2. The effective physical mass of the state for the lowest nonzero momentum for fixed bare masses ($m = M = 1$). (a) The dashed lines are perturbative approximations, showing that higher-order effects are significant at $\lambda = 0.7$. (b) Computed effective physical mass as a function of the cutoff momentum in the nonperturbative regime $\lambda = 0.7$ [$L = 0.01$. In (a), $P_{\max} = 3$, while in (b) $P_{\max}$ varies from 1 (leftmost) to 5 (rightmost). $N_b = 3$ and $N_{\rm fp} = 2$ for bosonic curves and $N_b = 2$ and $N_{\rm fp} = 2$ for fermionic curves].

are numerically stable at the 2% level for the parameters used in the figure. Since the nonperturbative regime requires larger Hilbert spaces, a smaller $P_{\max}$ must be chosen due to computational limitations, and along with a smaller $P_{\max}$ a smaller box length L must also be used. For $L = 0.01$, used in the figure, the box length is only slightly longer than the Compton wavelength, and for these short length scales the system is no longer Lorentz invariant. However, our results have suggested that this lack of Lorentz invariance only shows up in the energy of a particle at rest, as $\omega_k = \sqrt{(m^2c^4 + c^2k^2)}$ and $E_p = \sqrt{(M^2c^4 + c^2p^2)}$ turn out to fit all states except $p = 0$ (fermions) and $k = 0$ (bosons). Thus, for the nonperturbative regime we have chosen to define the mass by using the state with $p = 1$ (or $k = 1$), $m_{\rm phys} \equiv \sqrt{(\omega_1^2/c^4 - \Delta p^2/c^2)}$, and $M_{\rm phys} \equiv \sqrt{(E_1^2/c^4 - \Delta p^2/c^2)}$.

V. THE COMPUTATIONAL RENORMALIZATION SCHEME IN THE PERTURBATIVE REGIME

The ultraviolet divergences of the eigenvalues make the two Hamiltonians in their present forms useless and must be removed by a suitable renormalization program. Since the Yukawa theory in one spatial dimension is a renormalizable theory, only a finite number of bare parameters need to be computed to make every quantity divergence free. Here, we propose to renormalize the energies of the electron and boson at rest, which is equivalent to renormalizing their mass to the physically observed mass. Finally, we have to test whether the remaining physical quantities in the theory have become free of any divergences as well.

It is worth pointing out that there are two distinct notions of convergence which must be carefully distinguished from one another in this case. First, there is the issue of whether a theory is renormalizable at all or whether some divergence prevents the theory from being made finite at all. This issue is a currently unresolved issue for numerical work on quantum field theories, as there is the possibility that a very subtle divergence ruins renormalizability of the theory, but that the numerical accuracy is insufficient to resolve this divergence. The other kind of convergence which must be considered here is simple numerical convergence of the result. Of course, only if a theory is already known to be renormalizable, such as the Yukawa theory examined here, does it make sense to begin examining the theory numerically and to seek numerically converged results.

The Dirac Yukawa theory states $b_p^\dagger|0\rangle$ and $a_k^\dagger|0\rangle$, where $|0\rangle$ is the bare vacuum satisfying $b_p|0\rangle = a_k|0\rangle = 0$, represent virtual, nonphysical particle states that are not energy eigenstates of the fully coupled Hamiltonian H_D [Eqs. (2.3)]. Likewise, the Majorana theory states $f_p^\dagger|0\rangle$ and $a_k^\dagger|0\rangle$ are also not stable under the time evolution of H_M [Eqs. (2.6)]. Since a true physical (and stable) particle, which one would observe isolated from any other particles in a laboratory, does not change as a function of time, the Fock space states corresponding to a single physical particle (either fermion or boson) particle must be eigenstates of the Hamiltonians.

Here we must specify *stable* physical particle because in the Yukawa theory it is possible to construct unstable bosons; if the physical boson's mass is twice or more of the fermion's physical mass, then the boson can decay into two fermions. However, as long as we stay outside of this parameter regime, the physical boson is a stable particle and must be an eigenstate of the Hamiltonian.

Once the eigenstates corresponding to the single physical boson and fermion at rest have been identified, the energies of these states do not match the experimentally observed energies of these states, which are given by $m_{\rm phys}c^2$ for the photon and $M_{\rm phys}c^2$ for the electron, where $m_{\rm phys}$ and $M_{\rm phys}$ are the corresponding physical masses, respectively. For our model system here we arbitrarily require them to take the specific values $m_{\rm phys} = M_{\rm phys} = 1$. In order to obtain the correct physical energy, the bare mass parameters m and M must be adjusted to the proper value to yield the required physical masses. Here the photon's and electron's bare mass parameters must be chosen as functions of the momentum cutoff $\Lambda = P_{\max}\,\Delta p$. In fact, we show below that both of them have to be chosen to diverge as $\Lambda \to \infty$. The goal of the renormalization scheme is, for any given value of the cutoff

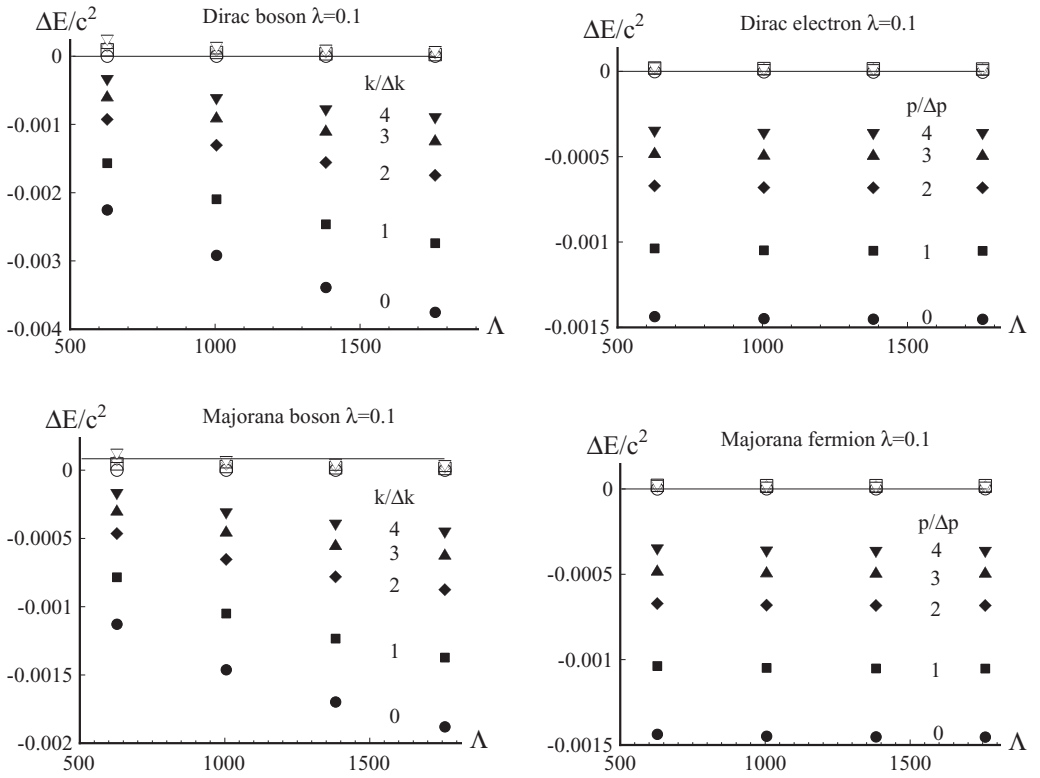

FIG. 3. Difference in energies ΔE between E_{num} and the corresponding required physical energy $\sqrt{({m_{\text{phys}}}^2\, c^4 + c^2\, p^2)}$ for the first five energy eigenvalues. The energies E_{num} obtained after the numerical renormalization scheme (based on m_∞ and M_∞) are the open markers. The original (unrenormalized) energies (based on our choice $m_1 = M_1 = 1$) are the closed markers. (a) The boson in the Dirac theory, (b) the Dirac electron, (c) the boson in the Majorana theory, and (d) the Majorana fermion. [Parameters are the required masses $m_{\text{phys}} = M_{\text{phys}} = 1$, $\lambda = 0.1$, and $L = 0.05$. For bosonic curves, $N_b = 2$, and $N_p = 1$, while for fermionic curves $N_b = 1$ and $N_{\text{fp}} = 1$. P_{max} ranges from 5 (leftmost) to 14 (rightmost)].

Λ, to find the $m(\Lambda)$ and $M(\Lambda)$ which yield $m_{\text{phys}} = M_{\text{phys}} = 1$ and then, once this is accomplished, to verify that other states in the spectrum have become Λ independent as well.

We have carried out the numerical renormalization program using an iterative approach. The initial "guess" for the bare mass parameters are just taken to be the physical masses, $m_0 = m_{\text{phys}}$, $M_0 = M_{\text{phys}}$. From these initial values, closer approximations to the correct bare parameters will be found iteratively, m_1 and M_1, m_2 and M_2, and so on. The photon's mass is updated, first, by using Newton's method: The physical mass of the photon is regarded as a function of the bare mass parameter, $m_{\text{phys}} = f(m)$, with all other parameters of the theory held constant, and then Newton's method is used to iteratively find the zeros of the function $f(m) - m_{\text{phys}}$. A single iteration of Newton's method is applied to the photon's bare mass to update it from m_0 to m_1. Since the photon and electron mass renormalizations are interdependent, the physical mass of the electron is calculated using a photon bare mass of m_1 and an electron bare mass of M_0, and from this an application of Newton's method similar to the one above is performed on the electron, yielding an updated electron mass M_1. The process can be repeated to calculate m_2 and M_2 from m_1 and M_1, and so on, as many times as necessary to achieve converged results. The final (optimum) bare parameters that lead to the correct physical masses (m_{phys} and M_{phys}) are denoted by m_∞ and M_∞, respectively.

In Fig. 3 we show the successful outcome of this iterative method applied to both the Dirac and Majorana Yukawa theories for a range of Λ values. Graphed in the figure is the difference in energy ΔE between the numerical energy eigenvalue E_{num} of various one-particle states, calculated using the numerical methods discussed in Sec. II, and the desired physical energy $\sqrt{({m_{\text{phys}}}^2\, c^4 + c^2\, p^2)}$ before ($m = M = 1$, filled symbol) and after ($m = m_\infty$, $M = M_\infty$, open symbols) the iterative renormalization,

$$\Delta E = E_{\text{num}}(p, m_\infty, M_\infty; \Lambda) - \sqrt{\left({m_{\text{phys}}}^2\, c^4 + c^2\, p^2\right)}. \quad (5.1)$$

Since the renormalization procedure is set up to ensure that the energy of a physical particle at rest, $p = 0$, becomes equal to $m_{\text{phys}}c^2$ for the boson and $M_{\text{phys}}c^2$ for the fermion, it is guaranteed that ΔE will be 0 for the zero-momentum mode $p = 0$ (circles). Fortunately, the other modes have also obtained negligable ΔE in comparison to the original energies. This indicates that the divergence has been successfully removed for all states in the single physical particle sector of the Fock space.

We have tried to fit the numerically obtained bare parameters as a function of Λ and found that for the Dirac theory

$$m(\Lambda) = 0.9929 + 0.0033 \ln \Lambda, \quad (5.2a)$$

$$M(\Lambda) = 1.0014, \quad (5.2b)$$

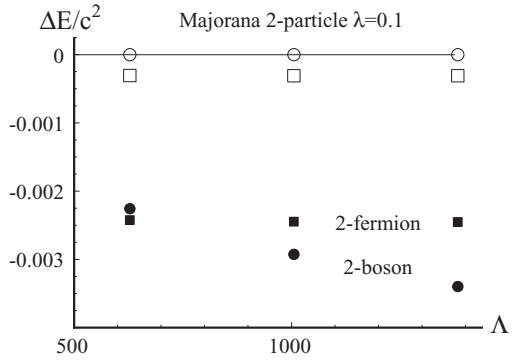

FIG. 4. Difference in energy ΔE between the calculated energy and the energy of two free particles with zero total momentum for the Majorana theory. Renormalized energies are open markers, unrenormalized energies are closed markers, the boson-boson state is represented by circles, and the fermion-fermion state by squares. [Parameters are $m_{\rm phys} = 1$, $M_{\rm phys} = 1$, $\lambda = 0.1$, and $L = 0.05$. For bosonic curves, $N_b = 3$, and $N_{\rm fp} = 1$, while for fermionic curves $N_b = 1$ and $N_{\rm fp} = 2$. $P_{\rm max}$ ranges from 5 (leftmost) to 11 (rightmost)].

while for the Majorana theory

$$m(\Lambda) = 0.9964 + 0.00075 \ln \Lambda, \tag{5.2c}$$

$$M(\Lambda) = 1.0014. \tag{5.2d}$$

These bare parameters lead to $m_{\rm phys} = M_{\rm phys} = 1$ for $\lambda = 0.1$ and $L = 0.05$.

VI. COMPUTATIONAL RENORMALIZATION OF CORRELATED TWO-PARTICLE ENERGIES IN THE PERTURBATIVE LIMIT

To complete the verification of the renormalization program, it is also necessary to show that the multiparticle states have also become divergence-free, which has been done in Fig. 4. Due to the large number of Fock space states involved, only the Majorana theory has been examined in Fig. 4. In the figure, we have graphed again the difference in energy ΔE between the numerically calculated energy and the lowest energy of the state for two *free (noninteracting)* particles and zero total momentum. For the two-boson state, two free particles with zero momentum have a total energy of $2m_{\rm phys}c^2$, while for two free fermions with zero momentum, the total energy is $2\sqrt{(M_{\rm phys}{}^2c^4 + c^2\Delta p^2)}$, since Pauli exclusion forces one fermion to take $p = \Delta p$ and the other $p = -\Delta p$ if the total momentum is to be zero. As seen in the figure, the energies of the zero-momentum two-particle states have also become free of divergences and independent of the cutoff Λ.

It should be noted that in our system the two physical particles can interact, and this may lead one to worry that a two-particle system might require also a divergent bare coupling constant λ. However, in a single spatial dimension, power-counting arguments suggest that the interaction vertex is superficially convergent. This means that, although the true physical coupling between the fermion and boson differs from the parameter λ that appears in the Hamiltonian, this shift is finite and an infinite renormalization is not necessary. Thus, the two-particle states in Fig. 4 can also be rendered divergence-free with only a mass renormalization with no need for an infinite bare coupling constant renormalization as well.

While, according to Fig. 4, it appears that the two-boson system has no noticeable interaction energy as ΔE is close to zero, the two-fermion system appears to have a smaller energy than the two free particles, suggesting an attractive interaction. Fortunately this energy is finite and does not depend on the cutoff Λ.

VII. SINGLE-PARTICLE ENERGIES IN THE NONPERTURBATIVE REGIME

The numerical renormalization procedure discussed here is fundamentally nonperturbative and differs from the usual order-by-order renormalization procedure. Figure 5 examines this method in the strong-coupling regime beyond lowest order in perturbation theory. Because the strong-coupling regime requires a larger number of Fock space states in order to converge, only the Majorana theory has been analyzed in this regime, as it has a smaller number of Fock space states due to the indistinguishability of the fermions as already mentioned above.

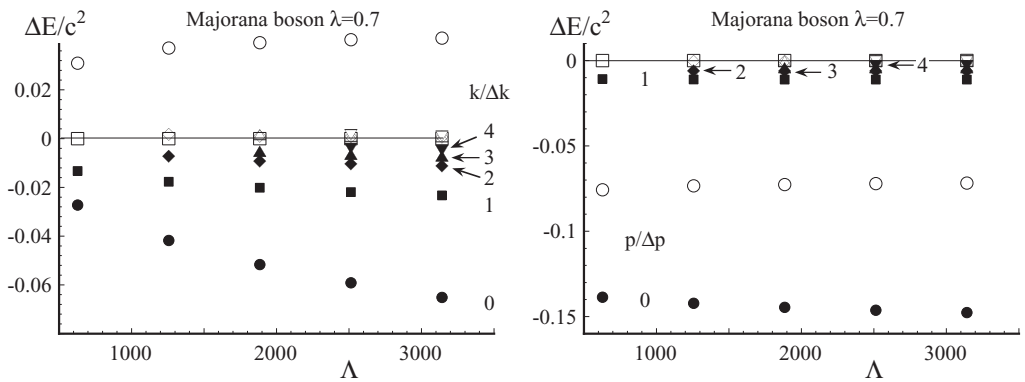

FIG. 5. Difference in energies ΔE between the numerically calculated energy eigenvalue and the physical energy $\sqrt{(m_{\rm phys}{}^2\, c^4 + c^2\, p^2)}$ in the nonperturbative regime. Renormalized energies are open markers and unrenormalized energies are closed markers. (a) The boson in the Majorana theory, while (b) is the Majorana fermion. [Parameters are $m_{\rm phys} = M_{\rm phys} = 1$, bare mass $m = M = 1$ for unrenormalized energies, $\lambda = 0.7$, and $L = 0.01$. For bosonic curves, $N_b = 3$, and $N_{\rm fp} = 2$, while for fermionic curves $N_b = 2$ and $N_{\rm fp} = 2$. $P_{\rm max}$ ranges from 1 (leftmost) to 5 (rightmost)].

For the boson, shown in Fig. 5(a), the renormalized single-particle energies of all of the nonzero momentum modes are quite close to their required physical values, in comparison to the unrenormalized energies. Furthermore, while the unrenormalized energy for each of the momentum modes depends on the cutoff Λ, the renormalized boson has become Λ independent, except for the $k = 0$ mode, showing that the infinities have been removed successfully for the nonzero momenta. We should note that, in this nonperturbative parameter regime, we have chosen to perform the renormalization procedure on bosons and fermions with momentum $p = 1$ (or $k = 1$), since the zero-momentum states are affected by the non-Lorentz invariance, as discussed prior to Fig. 2. Due to this lack of Lorentz invariance in the zero-momentum states, the renormalization of $k = 0$ is very poor in Fig. 5(a); this, however, is due to limitations of computational resources which prevented us from using larger box sizes L in this parameter regime, and not with any intrinsic problems with this renormalization scheme. The fermion, in Fig. 5(b), shows very similar results; the $p = 0$ mode encounters Lorentz invariance problems, but all of the other states in the theory are renormalized to their correct energies.

VIII. DISCUSSION AND OUTLOOK

In summary, we have proposed a new purely numerical method to remove any ultraviolet divergences from the energy eigenspectrum of a quantum field theoretical system. It is based on the Hamiltonian formulation of the system and used iterative techniques based on the repeated diagonalization to compute the (formally) diverging bare parameters that lead to the correct required physical quantities. The numerical solutions to quantum field theories presented here promise to provide a new tool for studying nonperturbative effects in quantum field theory, along with the additional advantage of being able to observe space- and time-resolved dynamics of field-theoretical systems. First steps have already been taken in this direction, and here we have shown that it is possible to incorporate renormalization techniques into these numerical solutions, a necessary step towards solving more complex theories such as QED that contain divergences that must be removed.

This new approach has several advantages but also disadvantages compared to the traditional approach. It does not rely on any perturbative expansions of complicated Green's functions, propagators, autocorrelation functions or Feynman diagrams and is, therefore, conceptually much easier to implement. However, the principal bottleneck of this brute-force method is the limitation due to computer memory. It requires new and more efficient Hilbert space truncation schemes to be applicable to more general three-dimensional systems such as full QED. The present work just serves as a proof of concept and we used a simplified version of the Yukawa theory in one spatial dimension with Dirac fermions and also with Majorana fermions.

There are, of course, a number of similarities between the numerical methods presented here and lattice gauge theories, and in particular, both regulate divergent integrals by placing the system on a grid which has a natural cutoff to the momentum modes. However, it must be noted that, while lattice gauge theory techniques are most useful for asymptotically free theories, our methods are equally useful for nonasymptotically free theories, such as QED. Furthermore, since the methods used here are based on diagonalization of a Hamiltonian, the eigenstates are recovered in addition to the eigenenergies, whereas one usually only obtains eigenenergies from lattice gauge theory techniques.

In the present study we have computed the energy eigenvalues by a direct numerical diagonalization of the Hamiltonian matrix. However, there are other methods (e.g., based on variational principles or imaginary time integration techniques) that could be explored to provide similar spectral information that is required in our method for renormalization. In the present approach we have used the eigenstates of the interaction-free part of the Hamiltonian as basis states. However, depending on the type of interaction more efficient (partly dressed) basis states can be identified.

In the interesting nonperturbative regime, many mathematical properties of renormalizable Hamiltonian matrices are not very well understood. For example, it is not known how the structure of the corresponding eigenvectors of the Hamiltonian is affected by the mass renormalization. These eigenvectors could become delocalized with respect to the basis of interaction-free states. This is an important issue in order to use spectral methods to compute the time evolution of arbitrary initial states. We should also note that nonperturbative techniques that permit us to examine whether a finite number of free parameters are sufficient to renormalize a Hamiltonian matrix are difficult to find.

As has been pointed out in the literature [30], many works deal with the question of the single-particle spectrum on an approximate level. It therefore is important to examine whether these approximations are fully consistent with the basic requirements of quantum field theory. For example, approximations to the spectral function, which is proportional to the imaginary part of the full retarded two-point correlation function, have to be analyzed very carefully for bosonic as well as fermionic quantum fields. In a recent work [31,32] it was shown that the requirement of causality (expressed as the vanishing anti- or commutators of field operators for spacelike separations) leads to mathematically rigorous constraints for the resummed propagators in high-temperature gauge theory [30,33].

In the model system examined here based on Dirac and also Majorana fermions, it is well known that the anticommutator of free as well as interacting field operators vanish for spacelike separations, which should imply that the corresponding Fourier transform of the spectral function into coordinate space in the continous limit should also vanish in this domain. However, in our work we are dealing exclusively with a finite Hilbert space, for which the generalization of the Lorentz invariance for a finite grid system is nontrivial in a mathematically rigorous way.

Furthermore, a distinction between causal and noncausal locality is much more complicated than in the continous limit. In fact, many interesting and fundamental question of quantum field theory on infinite Hilbert spaces are still open [3,30].

ACKNOWLEDGMENTS

We profited immensely from discussions with H. Matsuoka on the Schwinger models, QCD, and lattice gauge theory. We also thank C. C. Gerry, Y. T. Li, S. Meuren, C. Müller, A. Di Piazza, and E. V. Stefanovich for stimulating discussions. This work has been supported by the NSF and the NSFC (Grant No. 11128409).

APPENDIX

In this Appendix we compare the computational renormalization method with four different approaches. The first three are well established, but each of them has the drawback that it can be applied only in the perturbative weak-coupling limit, while higher-order terms are increasingly complicated. As there are numerous descriptions available in the literature, we just briefly summarize the four approaches below and apply them only to the Dirac model system for $\lambda = 0.1$. To have concrete numbers for a comparison below, for a box length $L = 0.05$ and momentum cutoff $\Lambda = 1380$ our bare parameters were computed as $m_b = 1.0034$ and $M_b = 1.0014$ in order to produce $m_{\rm phys} = 1$ and $M_{\rm phys} = 1$ for the perturbative coupling $\lambda = 0.1$. Because the photon's bare mass is divergent at first order, there could be an ambiguity when comparing different renormalization methods directly, since different methods may use different definitions of the regulation parameter Λ. Since the fermion's mass correction is finite at lowest order in perturbation theory, this ambiguity does not occur, and so we use the correction to the fermion mass below in order to compare various renormalization methods.

1. Spectral analysis based on bare Rayleigh-Schrödinger perturbation theory in λ

Conceptually, most similar to our approach would be to find the analytical expressions for the eigenenergies based on the usual perturbation theory [34] in λ. The resulting two expressions for the fermionic and bosonic single-particle rest energies as a function of M_b, m_b, λ, and Λ are then set equal to their required values $M_{\rm phys}c^2$ and $m_{\rm phys}c^2$, respectively. The resulting two coupled transcendental equations would then be solved (perturbatively) for a given cutoff momentum Λ in order to find the unknown parameters of the two bare masses M_b and m_b.

If we denote the unperturbed energy associated with the (bare) unperturbed state $|\alpha\rangle$ with E_α, then for states that satisfy $\langle\alpha|V|\alpha\rangle = 0$, the second-order eigenvalues take the general form $E_\alpha(\lambda) = E_\alpha + \langle\alpha|\alpha\rangle^{-1} \int d\beta\, |\langle\beta|V|\alpha\rangle|^2/(E_\alpha - E_\beta)$. The integration extends over all unperturbed states $|\beta\rangle$ that can contribute to the integral. The normalization factor $\langle\alpha|\alpha\rangle^{-1}$ is often omitted in the literature but is important for the continuous system as the single- and multiparticle states have different units and, therefore, different normalization properties. For systems with discrete spectra, however, all states can be normalized identically to the Kronecker δ and $\langle\alpha|\alpha\rangle^{-1}$ is always equal to 1.

More specifically, if we apply this technique to our system, the energy of a single fermion state with no momentum $|\alpha\rangle = |p = 0\rangle$ has energy $E_1(\lambda = 0.1) = 18\,639$ when the bare mass M_b is chosen to be 1. After the vacuum energy's contribution $E_0(\lambda = 0.1) = \langle 0|V|0\rangle = -113$ has been subtracted out, this implies that the mass of the particle is $(E_1 - E_0)/c^2 = 0.9986$, somewhat less than the desired value of $M_{\rm phys} = 1$. At these small, perturbative parameters, one could guess that the bare mass should be chosen to be $M_b = 1.0014$, which will give a perturbative energy that corresponds to the correct physical mass $M_{\rm phys} = 1$. This agrees perfectly with the numerical results above.

2. Two-point correlation function Feynman approach

This method is based on the observation that for any interacting quantum-field-theoretical system the Fourier transformed time-ordered two-point correlation function of the Heisenberg field operator $\phi(x,t) = \phi(X)$ in the physical vacuum state $|\text{Vac}\rangle$ has a single isolated pole if the square of the four-momentum P is equal to the physical mass of the particle.

$$\int dX\ \exp(iPX)\,\langle \text{Vac}|T\{\phi(x,t)\phi(x=0,t=0)\}|\text{Vac}\rangle = Z\,f(P)/\left(P^2 - {M_{\rm phys}}^2c^2\right) + \cdots . \tag{A1}$$

This correlation function is a central quantity in the field-based approach to relativistic quantum mechanics advocated in most textbooks [35–37]. Here the residue $f(P)$ depends on whether the particle is a fermion $[f(P) = i(\gamma^\mu p_\mu + Mc)]$ or a boson $[f(P) = i]$ and Z is the so-called "wave function normalization constant." In the special case of an interaction free system, we would find $Z = 1$.

Using Wick rotation and perturbative Feyman diagrams, one can find the corresponding expression for the left-hand side of Eq. (A1). We then choose M_b and m_b appropriately to guarantee that the poles of these expressions match the required ones given by the right-hand side of Eq. (A1). This step introduces the required values of $M_{\rm phys}c^2$ and $m_{\rm phys}c^2$.

More specifically, if we apply this technique to our system, we obtain for the lowest order loop correction to the fermion two-point function, defined as $-i\,\Sigma_{\rm loop}(p)$,

$$-i\,\Sigma_{\rm loop}(p) = \lambda^2/(4\pi)\,(-\gamma_\mu p^\mu/(M^2c^2)\ln(m/M) + 1/[mc^2\sqrt{(4M^2 - m^2)}][2Mc + \gamma_\mu p^\mu(2M^2 - m^2)/M^2] \times \{\tan^{-1}[-m/\sqrt{(4M^2 - m^2)}] - \tan^{-1}[(2M^2 - m^2)/\sqrt{(4M^2 - m^2)}/m]\}). \tag{A2}$$

The left-hand side of Eq. (A1) works out to be $i/[\gamma_\mu p^\mu - Mc - \Sigma_{\rm loop}(p)]$, accurate to lowest order in perturbation theory in λ, while the right-hand side can be rewritten as $iZ/(\gamma_\mu p^\mu - M_{\rm phys}c)$ for fermions. Equation (A1) can then be rewritten as

$$Z[\gamma_\mu p^\mu - Mc - \Sigma_{\rm loop}(p)] = (\gamma_\mu p^\mu - M_{\rm phys}c). \tag{A3}$$

The wave function renormalization term Z can be found be equating terms that contain $\gamma_\mu p^\mu$. The result, accurate to lowest order, is

$$Z = 1 + \lambda^2/(4\pi)\big(-1/\big({M_{\rm phys}}^2 c^2\big)\ln(m_{\rm phys}/M_{\rm phys}) + \big(2{M_{\rm phys}}^2 - {m_{\rm phys}}^2\big)/\big[m_{\rm phys}c^2{M_{\rm phys}}^2\sqrt{\big(4{M_{\rm phys}}^2 - {m_{\rm phys}}^2\big)}\big] \times\Big\{\tan^{-1}\big[-m_{\rm phys}/\sqrt{\big(4{M_{\rm phys}}^2 - {m_{\rm phys}}^2\big)}\big] - \tan^{-1}\big[\big(2{M_{\rm phys}}^2 - {m_{\rm phys}}^2\big)/\sqrt{\big(4{M_{\rm phys}}^2 - {m_{\rm phys}}^2\big)}/m_{\rm phys}\big]\Big\}\big). \quad \text{(A4)}$$

Here the bare masses m and M have been simply replaced by the physical masses $m_{\rm phys}$ and $M_{\rm phys}$, because these masses differ only by terms proportional to λ^2, and the entire term they appear in is already of that order. Equating the momentum-independent terms in Eq. (A3) then gives an equation for the bare mass M, which can be found to lowest order in perturbation theory to be

$$M = M_{\rm phys} + \lambda^2/(4\pi c)\big(1/(M_{\rm phys}c)\ln(m_{\rm phys}/M_{\rm phys}) + \sqrt{\big(4{M_{\rm phys}}^2 - {m_{\rm phys}}^2\big)}/(m_{\rm phys}M_{\rm phys}c) \times\Big\{\tan^{-1}\big[-m_{\rm phys}/\sqrt{\big(4{M_{\rm phys}}^2 - {m_{\rm phys}}^2\big)}\big] - \tan^{-1}\big[\big(2{M_{\rm phys}}^2 - {m_{\rm phys}}^2\big)/\sqrt{\big(4{M_{\rm phys}}^2 - {m_{\rm phys}}^2\big)}/m_{\rm phys}\big]\Big\}\big). \quad \text{(A5)}$$

For the required parameters ($\lambda = 0.1$ and $m_{\rm phys} = M_{\rm phys} = 1$), the bare mass of the fermion works out to be $M = 1.0014$, again in agreement with the numerical result above.

3. Renormalized perturbation theory based on counterterms

In this approach, one tries to incorporate from the very beginning the required physical parameters and also physical operators into the original Hamiltonian $H(\mu_b, \mathrm{O}_b)$. To shorten our notation, the symbol μ_b represents all bare parameters (m and M for our specific models) and O_b represents the group of all field operators (ϕ_b and ψ_b for our Hamiltonians). In order to include these quantities it is necessary to assume that the bare field operator O_b is simply a multiple of the physical (often called "renormalized") field operator, $O_b = Z^{1/2}\, O_{\rm phys}$. This important assumption allows us to eliminate O_b entirely from H, but at the same time introduces a new unknown parameter Z into the approach. Its numerical value is determined by the residue (numerator) of the terms on the right-hand side of Eq. (A1). After this necessary rescaling, the original Hamiltonian can then be rewritten in the form

$$H(\mu_b, O_b, \lambda) = H(\mu_{\rm phys}, O_{\rm phys}, \lambda) + C(\mu_b, \mu_{\rm phys}, O_{\rm phys}, Z, \lambda). \quad \text{(A6)}$$

These counterterms $C(\mu_b, \mu_{\rm phys}, O_{\rm phys}, Z, \lambda)$ typically diverge in Λ to permit the entire Hamiltonian to lead to a finite spectrum. Furthermore, due to the different way of splitting up the various terms in H, a new set of Feynman rules can be constructed. These renormalized Feynman rules are then used to simplify perturbatively the expression for the two-point autocorrelation function shown in Eq. (A1).

If we apply this technique for our case, we find that the lowest-order correction to the two point function is $-i\,\Sigma(p) = -i\,\Sigma_{\rm loop}(p) + i\,\gamma_\mu p^\mu\,\delta z - i\,\delta m\,c$, where δz and δm are the coefficients of the wave function renormalization and mass counterterms, respectively, and now $\Sigma_{\rm loop}(p)$ must be evaluated using the physical masses $m_{\rm phys}$ and $M_{\rm phys}$. Because we are using counterterms, the mass appearing in the Feynman diagram propagators is now $M_{\rm phys}$, so instead of Eq. (A3) we get

$$\gamma_\mu p^\mu - M_{\rm phys}c - \Sigma(p) = (\gamma_\mu p^\mu - M_{\rm phys}c). \quad \text{(A7)}$$

The renormalization condition simply means that $\Sigma(p)$ must vanish. Equating terms proportional to $\gamma_\mu p^\mu$ gives an equation for δz, which is similar to Eq. (A4),

$$\delta z = \lambda^2/(4\pi)\big(-1/\big({M_{\rm phys}}^2 c^2\big)\ln(m_{\rm phys}/M_{\rm phys}) + \big(2{M_{\rm phys}}^2 - {m_{\rm phys}}^2\big)/\big[m_{\rm phys}c^2{M_{\rm phys}}^2\sqrt{\big(4{M_{\rm phys}}^2 - {m_{\rm phys}}^2\big)}\big] \times\Big\{\tan^{-1}\big[-m_{\rm phys}/\sqrt{\big(4{M_{\rm phys}}^2 - {m_{\rm phys}}^2\big)}\big] - \tan^{-1}\big[\big(2{M_{\rm phys}}^2 - {m_{\rm phys}}^2\big)/\sqrt{\big(4{M_{\rm phys}}^2 - {m_{\rm phys}}^2\big)}/m_{\rm phys}\big]\Big\}\big). \quad \text{(A8)}$$

Equating terms which are independent of the momentum then gives

$$\delta m = \lambda^2/(4\pi c)\big(1/(M_{\rm phys}c)\ln(m_{\rm phys}/M_{\rm phys}) + \sqrt{\big(4{M_{\rm phys}}^2 - {m_{\rm phys}}^2\big)}/(m_{\rm phys}M_{\rm phys}c) \times\Big\{\tan^{-1}\big[-m_{\rm phys}/\sqrt{\big(4{M_{\rm phys}}^2 - {m_{\rm phys}}^2\big)}\big] - \tan^{-1}\big[\big(2{M_{\rm phys}}^2 - {m_{\rm phys}}^2\big)/\sqrt{\big(4{M_{\rm phys}}^2 - {m_{\rm phys}}^2\big)}/m_{\rm phys}\big]\Big\}\big). \quad \text{(A9)}$$

Comparison of Eqs (A8) and (A9) with (A4) and (A5) then shows that this result is identical to the result of Sec. II.

4. Stefanovich renormalization approach based on zero self-scattering conditions

For completeness we should also briefly mention that there is a fourth method for renormalization which has been proposed recently by Stefanovich [38–40]. Similarly to the renormalized perturbation theory approach, the starting point here is the *interaction-free* part of the original Hamiltonian, where each bare parameter or operator has been replaced from the very beginning by its physical counterpart, $H = H_0(\mu_{\rm phys}, O_{\rm phys}, \lambda)$. The goal is then to add appropriate additional interaction terms $\Sigma_i\, c_i\, V_i$ to the Hamiltonian, such that the corresponding S-matrix in all perturbative orders

remains cluster separable, relativistic invariant, the physical masses of the particles are preserved and that it satisfies the so-called "no-self scattering" requirements. Here, no-self-scattering means that the S matrix carries the vacuum and the single-particle states into themselves, $\langle 0|\, S\, |0\rangle = 1$ and $\langle q'|\, S\, |q\rangle = \delta(q - q')$, where the state $|q\rangle$ is given by $|q\rangle \equiv \hat{a}^{\dagger}(q)|0\rangle$ and $|0\rangle$ denotes the vacuum state. The unknown expansion coefficients c_i are usually determined perturbatively. For a concrete application of this alternative method to a model potential, see Ref. [41].

[1] W. Thirring, Ann. Phys. **126**, 154 (1958).
[2] I. Bialynicki-Birula and Z. Bialynickia-Birula, *Quantum Electrodynamics* (Pergamon Press, Oxford, 1975).
[3] J. Glimm and A. Jaffe, *Quantum Physics* (Springer-Verlag, New York, 1981).
[4] D. Buchholz, Commun. Math. Phys. **85**, 49 (1982).
[5] R. Haag, *Local Quantum Physics* (Springer Verlag, Berlin, 1992).
[6] J. C. Baez, I. E. Segal, and Z. Zhou, *Introduction to Algebraic and Constructive Quantum Field Theory* (Princeton University Press, Princeton, NJ, 1992).
[7] H. Araki, *Mathematical Theory of Quantum Fields* (Oxford University Press, Oxford, 1999).
[8] C. C. Gerry and P. L. Knight, *Introductory Quantum Optics* (Cambridge University Press, Cambridge, 2004).
[9] For a recent review, see A. Di Piazza, C. Müller, K. Z. Hatsagortsyan, and C. H. Keitel, Rev. Mod. Phys. **84**, 1177 (2012).
[10] W. Greiner, B. Müller and J. Rafelski, *Quantum Electrodynamics of Strong Fields* (Springer-Verlag, Berlin, 1985).
[11] S. Weinberg, *The Quantum Theory of Fields*, Vol. 1 (Cambridge University Press, Cambridge, UK, 1995).
[12] M. Ligare and R. Oliveri, Am. J. Phys. **70**, 58 (2002).
[13] R. E. Wagner, M. R. Ware, B. T. Shields, Q. Su, and R. Grobe, Phys. Rev. Lett. **106**, 023601 (2011).
[14] R. E. Wagner, M. R. Ware, Q. Su, and R. Grobe, Phys. Rev. A **82**, 032108 (2010).
[15] R. E. Wagner, Q. Su, and R. Grobe, Phys. Rev. A **82**, 022719 (2010).
[16] R. E. Wagner, S. Acosta, S. A. Glasgow, Q. Su, and R. Grobe, J. Phys. A **45**, 275303 (2012).
[17] T. Cheng, E. R. Gospodarczyk, Q. Su, and R. Grobe, Ann. Phys. **325**, 265 (2010).
[18] P. Roman, *Introduction to Quantum Field Theory* (John Wiley & Sons, New York, 1969).
[19] L. H. Ryder, *Quantum Field Theory* (Cambridge University Press, Cambridge, 1985).
[20] V. Rivasseau, *From Perturbative to Constructive Renormalization* (Princeton University Press, Princeton, NJ, 1991).
[21] J. Collins, *Renormalization* (Cambridge University Press, Cambridge, 2003).
[22] B. Delamotte, Am. J. Phys. **72**, 170 (2004).
[23] F. Mandl and G. Shaw, *Quantum Field Theory* (Wiley, Chichester, 2006).
[24] R. Brunetti, M. Dütsch, and K. Fredenhagen, Adv. Theor. Math. Phys. **13**, 1541 (2009).
[25] J. Klauder, J. Phys. A **44**, 273001 (2011).
[26] P. A. Henning, Nucl. Phys. A **546**, 653 (1992).
[27] M. Kaku, *Quantum Field Theory* (Oxford University Press, Oxford, 1993).
[28] T. Morii, C. S. Lim, and S. N. Mukherjee, *The Physics of the Standard Model and Beyond* (World Scientific, Singapore, 2004).
[29] I. Montvay and G. Münster, *Quantum Fields on a Lattice* (Cambridge University Press, Cambridge, 1994).
[30] P. A. Henning, Phys. Rep. **253**, 235 (1995).
[31] P. A. Henning, Z. Phys. A **345**, 227 (1993).
[32] P. A. Henning, E. Poliatchenko, T. Schilling, and J. Bros, Phys. Rev. D **54**, 5239 (1996).
[33] H. Narnhofer, M. Requardt, and W. Thirring, Comm. Math. Phys. **92**, 247 (1983).
[34] A. Messiah, *Quantum Mechanics*, Vol. II (Noth-Holland, Amsterdam, 1966).
[35] S. S. Schweber, *An Introduction to Relativistic Quantum Field Theory* (Harper & Row, New York, 1962).
[36] M. E. Peskin and D. V. Schroeder, *An Introduction to Quantum Field Theory* (Westview Press, Boulder, 1995).
[37] M. Srednicki, *Quantum Field Theory* (Cambridge University Press, Cambridge, 2007).
[38] E. V. Stefanovich, Ann. Phys. **292**, 139 (2001).
[39] E. V. Stefanovich, arXiv:physics/0504062v13 [physics.gen-ph].
[40] E. V. Stefanovich, arXiv:hep-th/0503076 (2005).
[41] E. V. Stefanovich, R. E. Wagner, Q. Su, and R. Grobe, Laser Phys. **23**, 035302 (2013).